Available online at www.sciencedirect.com
ScienceDirect
Journal of the European Ceramic Society 29 (2009) 2097–2103
www.elsevier.com/locate/jeurceramsoc

Effect of Al dopant on the hydrothermal oxidation behavior of Ti_3SiC_2 powders

H.B. Zhang [a], X. Wang [a], C. Berthold [a], K.G. Nickel [a,*], Y.C. Zhou [b]

[a] *Applied Mineralogy, Institute for Geosciences, Eberhard-Karls-University Tübingen, Wilhelmstrasse 56, D-72074 Tübingen, Germany*
[b] *Shenyang National Laboratory for Materials Science, Institute of Metal Research, Chinese Academy of Sciences, Shenyang 110016, PR China*

Received 22 October 2008; received in revised form 2 December 2008; accepted 4 December 2008
Available online 20 January 2009

Abstract

Experimental and thermodynamic studies of the hydrothermal oxidation behavior of $Ti_3Si_{0.9}Al_{0.1}C_2$ powders were performed at 500–700 °C under a hydrostatic pressure of 50 MPa. Titanium, silicon and aluminum were selectively extracted from $Ti_3Si_{0.9}Al_{0.1}C_2$ during hydrothermal oxidation, resulting in the formation of oxides and disordered carbon. A comparative investigation with Ti_3SiC_2 disclosed the evident influence of Al dopant on the hydrothermal oxidation process, i.e. delaying the phase transformation from anatase to rutile, promoting the formation of carbon, the crystallization of silica and decomposition of $Ti_3Si_{0.9}Al_{0.1}C_2$. The corresponding mechanism was discussed.
© 2008 Elsevier Ltd. All rights reserved.

Keywords: Carbides; Hydrothermal oxidation

1. Introduction

Because advanced ceramics have demonstrated impressive chemical resistance at high temperatures, it is often inferred that they should be invulnerable to corrosion at relatively low temperatures. But this is not really true under hydrothermal conditions.[1] Attack of aggressive aqueous media can deteriorate ceramics even at 150 °C.[1] Under supercritical conditions, water is a corrosion medium and dangerous to advanced ceramics, because it can dissolve formed oxides during hydrothermal oxidation. Since advanced ceramics have been attracting great attention in energy related systems, where high-temperature and high-pressure water is usually involved, the hydrothermal oxidation behavior of silicon carbide,[2–7] silicon nitride[8–10] and alumina[11] has been investigated.

Ti_3SiC_2 has turned out to be an excellent structural/functional ceramic due to its combination of numerous salient properties of both metals and ceramics. This ceramics is expected to be a prospective material applied in energy related systems because it is machinability,[12,13] damage tolerance[14,15] and reliability.[16] Thus, the hydrothermal oxidation behavior of Ti_3SiC_2 is of great concern. The interaction of H_2O with Ti_3SiC_2 powders has been investigated at 500–700 °C under the pressure of 50 MPa.[17] The primary results shows that Ti and Si are selectively oxidative extracted from Ti_3SiC_2, resulting in the formation of TiO_2, SiO_2 and amorphous carbon.

Doping Al in Ti_3SiC_2 can form $Ti_3Si_xAl_{1-x}C_2$ solid solutions.[18] Even small amounts of Al dopant can significantly improve the oxidation resistance of Ti_3SiC_2.[18,19] For instance, $Ti_3Si_{0.9}Al_{0.1}C_2$ displays excellent oxidation resistance due to the formation of a continuous α-Al_2O_3 layer during oxidation.[18,19] Since the oxidation behavior of Ti_3SiC_2 is greatly influenced by adding Al dopant, it is very necessary to understand the effect of Al dopant on the hydrothermal behavior, which has not been investigated up to now.

In this work, the hydrothermal oxidation behavior of $Ti_3Si_{0.9}Al_{0.1}C_2$ powders in distilled water was investigated. A comparative study with Ti_3SiC_2 is also carried out at the similar conditions.

2. Experimental

The equilibrium reaction products were calculated using the FactSage 5.4 Gibbs free energy minimization program.[20] The database did not contain data for the $Ti_3Si_{0.9}Al_{0.1}C_2$ phase. The calculations were performed for a closed system with a constant

* Corresponding author. Tel.: +49 7071 2976802; fax: +49 7071 293060.
E-mail address: klaus.nickel@uni-tuebingen.de (K.G. Nickel).

0955-2219/$ – see front matter © 2008 Elsevier Ltd. All rights reserved.
doi:10.1016/j.jeurceramsoc.2008.12.010

total pressure of 50 MPa. The gas phases were assumed to be ideal, and the solid phases were treated as a mechanical mixture with unit activities. All possible gases were considered including hydrocarbons, hydroxyl species and volatile metal oxides. Only the major species are given in the final results.

The $Ti_3Si_{0.9}Al_{0.1}C_2$ powders were obtained by rasping the as-prepared bulk $Ti_3Si_{0.9}Al_{0.1}C_2$ specimen on a diamond file, and then grinding it in an agate muller. The bulk $Ti_3Si_{0.9}Al_{0.1}C_2$ was fabricated by the solid–liquid reaction synthesis and simultaneous *in situ* hot-pressing process,[21] which has been described elsewhere.[18] Briefly, this material was prepared according to the following procedure: mixed powders of Ti, Si, Al and graphite with near stoichiometric proportion were milled for 20 h in a polyurethane mill. After ball milling and drying, the powders were cold-pressed into a disc with 50 mm diameter in a graphite die. The preparation was conducted under an Ar atmosphere in a furnace using graphite as a heating element. The synthesis temperature was 1550 °C and the hot-pressing pressure was 38 MPa.

The $Ti_3Si_{0.9}Al_{0.1}C_2$ powders and distilled water were placed into gold capsules with 3 mm diameter and 30 mm length. Typically, a capsule contained 50 mg $Ti_3Si_{0.9}Al_{0.1}C_2$ powders and 75 mg distilled water (H_2O:$Ti_3Si_{0.9}Al_{0.1}C_2$ molar ratio of 16:1). After sealing by welding, these capsules were placed in tube-type pressure vessels made of René 41 superalloy. The experiments were carried out at 500–700 °C under a hydrostatic pressure of 50 MPa.

After oxidation, the powders were analyzed by XRD (Bruker, England, Co Kα radiation) and Raman spectroscopy (LabRam micro-Raman spectrometer, Dilor, France, excitation at 514.5 nm using Ar-ion laser).

3. Results

3.1. Reaction thermodynamics

Fig. 1(a) and (b), respectively, illustrates the equilibrium partial pressures of the gaseous products and the equilibrium amounts of solid species with different H_2O:$Ti_3Si_{0.9}Al_{0.1}C_2$ molar ratio at 700 °C and 50 MPa. The primary gaseous phases are hydrogen and methane, even for small amounts of water. The amounts of CO and CO_2 are quite low if there is not enough water, but they increase significantly with increasing water amount (Fig. 1(a)). For the solid products, insufficient amount of water results in the formation of titanium sub-oxides, and they transform to TiO_2 (rutile) as exceeding the minimum value of 7 mol H_2O per 1 mol the carbide (Fig. 1(b)). SiO_2 (quartz) is a persistent product and can remain stable almost in the whole water range. Aluminum is predicted to be oxidized as Al_2SiO_5 (sillimanite).

Fig. 2 shows the temperature-dependent partial pressures of the volatile compounds for a H_2O:$Ti_3Si_{0.9}Al_{0.1}C_2$ molar ratio of 16:1 under the pressure of 50 MPa. The mainly volatile phases are estimated as H_2O, H_2, CH_4, CO_2 and CO at the equilibrium state. Hydrogen and methane are the dominating gaseous products at 400–1000 °C, even though methane decreases with temperatures to yield more hydrogen and carbon oxides.

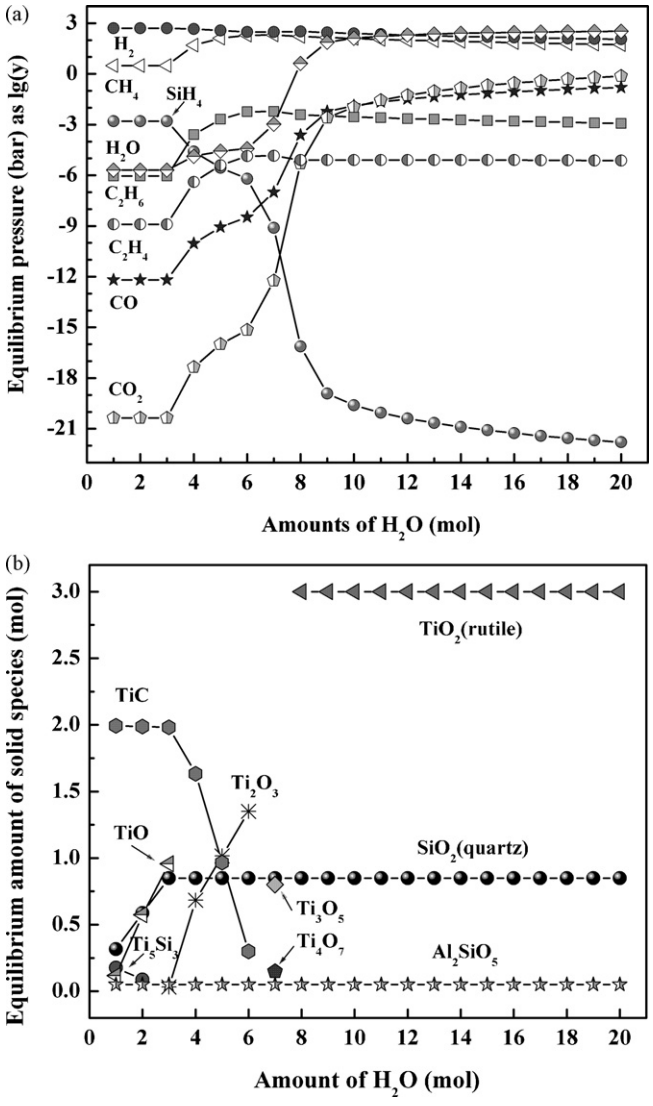

Fig. 1. (a) Equilibrium partial pressures of the gaseous products and (b) equilibrium amounts of solid species with different H_2O:$Ti_3Si_{0.9}Al_{0.1}C_2$ molar ratio at 700 °C under the pressure of 50 MPa.

3.2. Powder X-ray diffraction

X-ray diffraction patterns of $Ti_3Si_{0.9}Al_{0.1}C_2$ powders after hydrothermal oxidation are displayed in Fig. 3. The corresponding results of Ti_3SiC_2 powders are shown in Fig. 4. For $Ti_3Si_{0.9}Al_{0.1}C_2$, the product is identified as anatase at 500 °C and both anatase and rutile at 600–700 °C. Meanwhile, the amount of rutile increases with treatment time and temperatures, which is due to the phase transformation from anatase to rutile. No diffraction peaks of any Si-bearing phases are detected at 500–600 °C, but cristobalite occurs after treatment at 700 °C and its peaks are more evident with treatment time. A sillimanite peak is present at 700 °C after treatment for 90 h.

The detail explanation about the XRD of Ti_3SiC_2 powders after hydrothermal treatment can be found in Ref. 17. Here we only compare Ti_3SiC_2 with the new data (Fig. 4). The following changes are obvious after adding Al dopant:

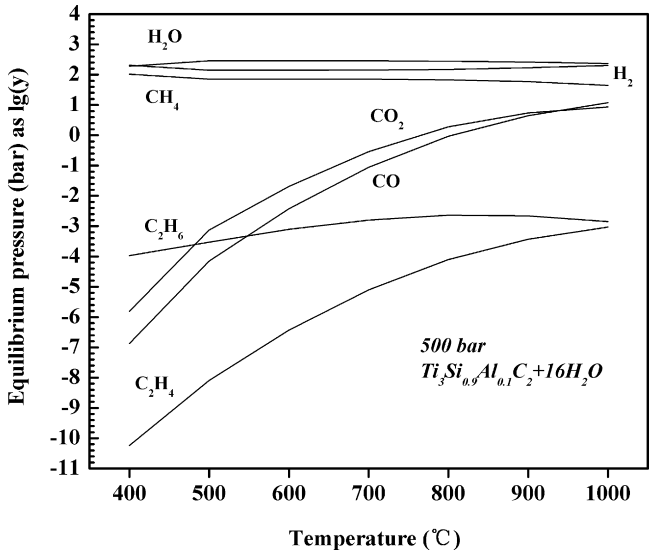

Fig. 2. Temperature-dependent partial pressures of the volatile compounds for a H_2O:$Ti_3Si_{0.9}Al_{0.1}C_2$ molar ratio of 16:1 under the pressure of 50 MPa.

(1) Delaying the phase transformation from anatase to rutile (Fig. 3(f) and (g) vs. Fig. 4(f) and (g)).
(2) Accelerating the crystallization of SiO_2 to form cristobalite (Fig. 3(f) vs. Fig. 4(f)).
(3) Promoting the decomposition of the carbide (Fig. 3(b) vs. Fig. 4(b)). Ti_3SiC_2 could sustain a treatment at 500 °C for 24 h, where $Ti_3Si_{0.9}Al_{0.1}C_2$ disappeared already after 20 h.

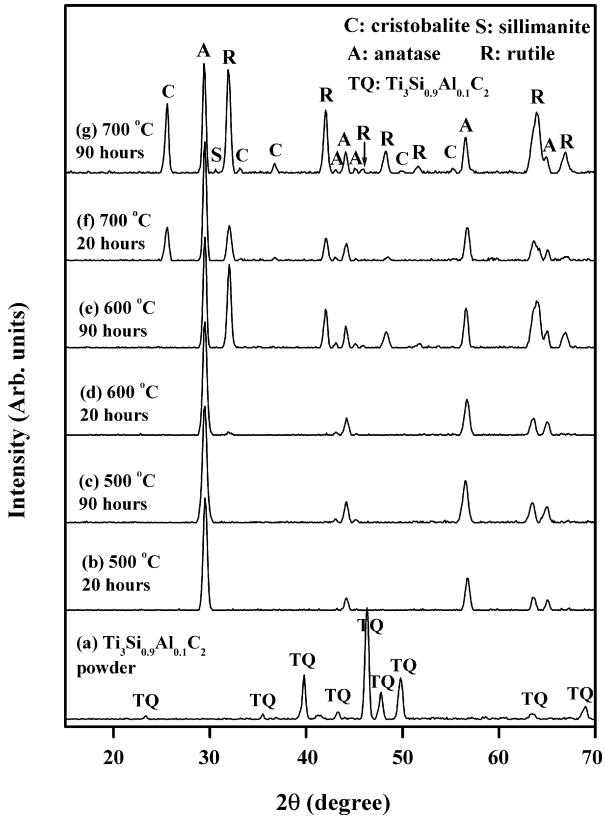

Fig. 3. XRD patterns of $Ti_3Si_{0.9}Al_{0.1}C_2$ powders after hydrothermal oxidation at 500–700 °C under the pressure of 50 MPa.

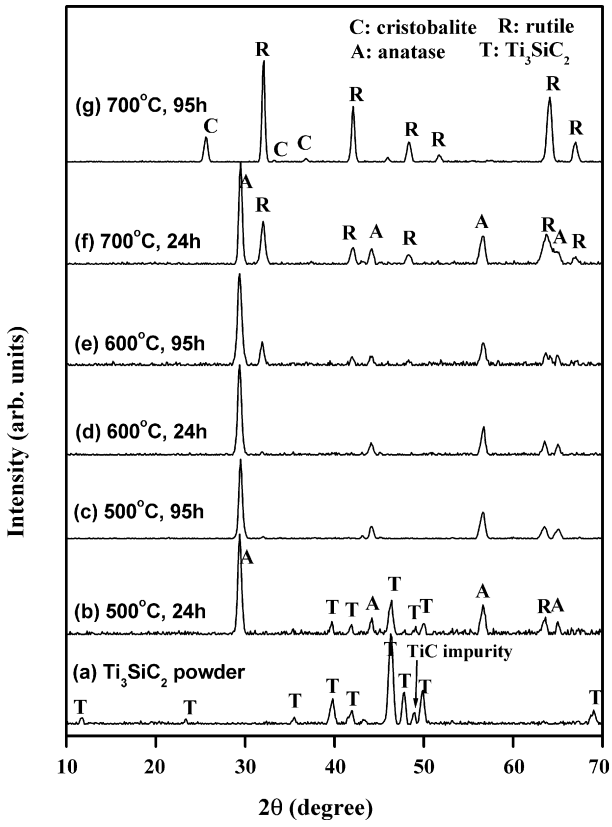

Fig. 4. XRD patterns of Ti_3SiC_2 powders after hydrothermal oxidation at 500–700 °C under the pressure of 50 MPa.

3.3. Raman spectroscopy

Raman spectroscopy is very useful to identify carbon allotropes[22,23] and is used to interpret structural characteristics.[24] The evolution of carbon, therefore, is analyzed using Raman spectroscopy (Fig. 5). After hydrothermal oxidation, the Raman spectra clearly show strong bands of the graphite band (G) and the disordered/nanocrystalline carbon band (D),[1–5] which give evidence of carbon formation. The amounts of as-formed carbon, however, remarkably decrease with treating time (Fig. 5(e) and (f)) due to the reaction with water. The observed up-shift of the D band indicates that the bond-angle disorder of carbon is decreased with temperatures and treatment time.[1] Little carbon is produced after hydrothermal treatment of Ti_3SiC_2 at 500 °C for 24 h (Fig. 6); however, amounts of carbon present for $Ti_3Si_{0.9}Al_{0.1}C_2$ at the similar conditions. This result suggests the promotion effect of aluminum dopant for producing carbon.

4. Discussions

4.1. Products after hydrothermal treatment

Concerning the $Ti_3Si_{0.9}Al_{0.1}C_2$ powders, the solid products after the hydrothermal oxidation are oxides and carbon. Because rutile is more stable than anatase,[25,26] the first formed anatase transforms into rutile. This phase transformation has also been observed in the hydrothermal oxidation of

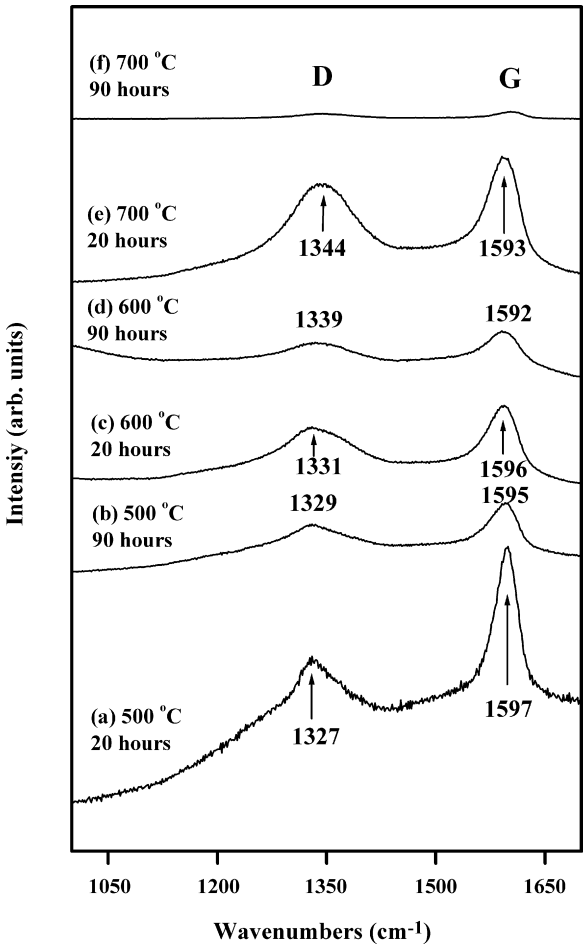

Fig. 5. Raman spectra of $Ti_3Si_{0.9}Al_{0.1}C_2$ powders after hydrothermal treatment at 500–700 °C under the pressure of 50 MPa.

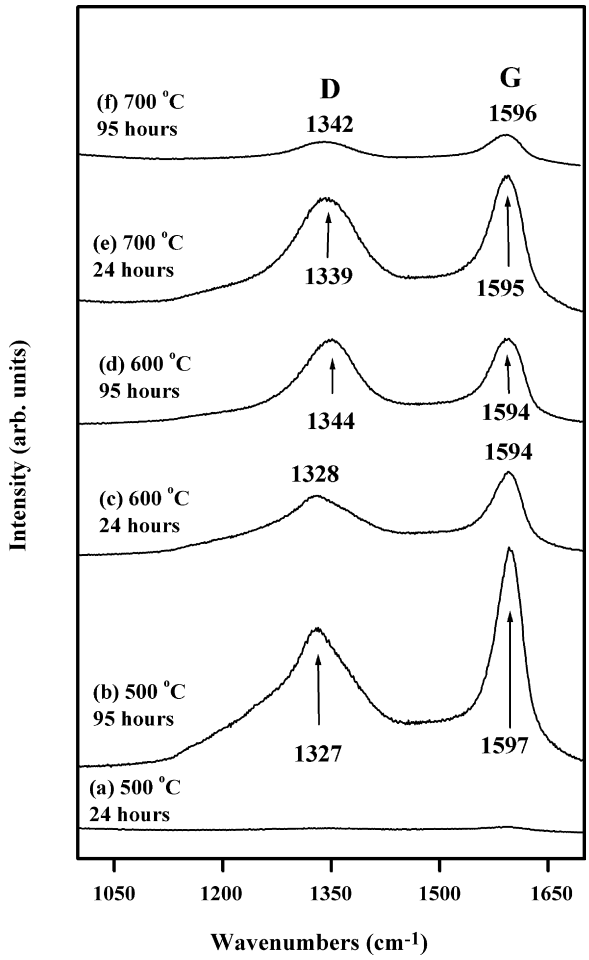

Fig. 6. Raman spectra of Ti_3SiC_2 powders after hydrothermal treatment at 500–700 °C under the pressure of 50 MPa.

Ti_3SiC_2 powders[17] and the intermediate temperature oxidation of Ti_3SiC_2.[27] The detail influences (grain size, impurities, etc.) on this sluggish transformation have been investigated in other powder studies.[28] Cristobalite occurs at 700 °C, and at 500–600 °C the absence of the XRD patterns of crystalline SiO_2 is attributed to the formation of amorphous silica. This is consistent with the previous investigations on the hydrothermal behavior of Ti_3SiC_2.[17] During the oxidation of Ti_3SiC_2 in air/oxygen, SiO_2 appears as amorphous,[29–33] tridymite,[34] or cristobalite[29,32,33,35,36] in different studies, which originates from the different microstructure, density and purity of each sample tested. Besides sillimanite, the existence of amorphous Al_2O_3 cannot be excluded considering the high stability of Al_2O_3 and the formation of amorphous Al_2O_3 in the oxidation of bulk $Ti_3Si_{0.9}Al_{0.1}C_2$ at 500–700 °C in air.[37]

Similar to Ti_3SiC_2,[17] carbon is produced after the hydrothermal treatment. The formed carbon can be described as disordered carbon according to the combination results of Raman and XRD. Carbon is not found on the gold capsule walls after experiments, so the carbon rather formed by oxidation extraction of titanium, silicon and aluminum out of the carbide than by deposition out of the fluid. The factors of both thermodynamics and kinetics contribute to the formation of carbon. Of them, kinetics plays an essential role on this process because the existence form of C, indicated by the thermodynamic calculations, should be methane and carbon oxides, and TiC at the condition of insufficient water.

From the point of view of thermodynamics, the affinity of metals to oxygen is much higher than that of carbon,[3,38,39] resulting in the formation of TiO_2, SiO_2 and sillimanite and the survival of carbon from oxidation. Owing to the similar reason, carbon is produced after hydrothermal treatment and oxidation of transition metal carbides.[3,38,39]

From the point of view of kinetics, the formation of carbon is related to the unique characteristics of the solid solution: (1) $Ti_3Si_{0.9}Al_{0.1}C_2$ possesses the similar layered structure as Ti_3SiC_2 and Ti_3AlC_2[18,40] and (2) the bonds of Ti–Si and Ti–Al are weaker than those of Ti–C.[41] These weak bonds and layered structure of grains lead to the high activity and easy diffusion of aluminum and silicon, which has been proved by the oxidation[18,19] and thermal stability testing of $Ti_3Si_{0.9}Al_{0.1}C_2$.[42] In addition, the layered structure is favourable for the diffusion of oxygen, which facilitates the oxidation of titanium. The fast diffusion of gas species has been observed in the "Ti_3SiC_2 pest" phenomenon.[43] Therefore, titanium, aluminum and silicon can be selectively removed from the substrate through oxidation, which leads to the formation of carbon.

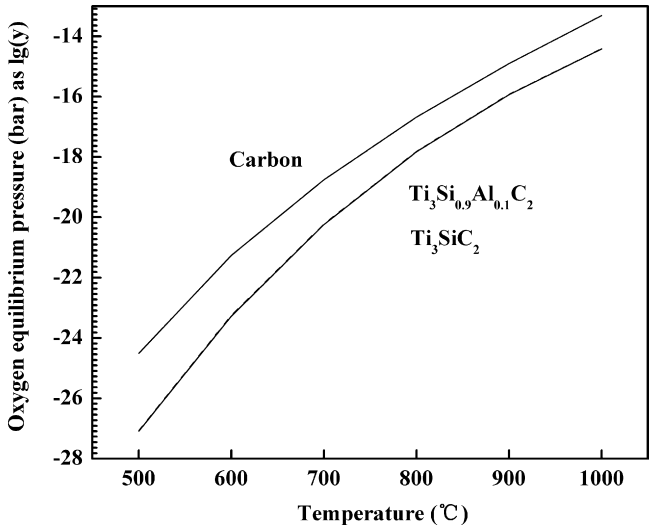

Fig. 7. Equilibrium oxygen partial pressure under the conditions of 500–1000 °C and the hydrostatic pressure of 500 bar. The FactSage 5.4 program was used for the calculations. The chosen systems were respectively 1 mol Ti_3SiC_2 + 16 mol H_2O, 1 mol $Ti_3Si_{0.9}Al_{0.1}C_2$ + 16 mol H_2O and 1 mol C + 8 mol H_2O.

Fig. 7 displays the calculated oxygen partial pressure under the conditions of 500–1000 °C and the hydrostatic pressure of 500 bar. For Ti_3SiC_2 and $Ti_3Si_{0.9}Al_{0.1}C_2$, the oxygen partial pressures in the environments are quite similar and range from 10^{-28} to 10^{-15} bar. The values for the existence of free carbon are calculated to be 10^{-25} to 10^{-14} bar. This explains both the possibility of the formation of free carbon and its vanishing after some time, because high C:H_2O ratios favour higher oxygen partial pressures and hence the removal as carbon oxides.

4.2. Hydrothermal oxidation process of $Ti_3Si_{0.9}Al_{0.1}C_2$

The hydrothermal oxidation of $Ti_3Si_{0.9}Al_{0.1}C_2$ displays a two-step process. At the first stage, $Ti_3Si_{0.9}Al_{0.1}C_2$ reacts with H_2O to produce TiO_2, SiO_2, Al_2SiO_5 and carbon. For an exact balance with a complete transformation to the oxides the corresponding reactions are

$$Ti_3Si_{0.9}Al_{0.1}C_2 + 7.95H_2O = 3TiO_2 + 0.85SiO_2 + 0.05Al_2SiO_5 + 2C + 7.95H_2 \quad (1)$$

and

$$Ti_3Si_{0.9}Al_{0.1}C_2 + 7.95H_2O = 3TiO_2 + 0.85SiO_2 + 0.05Al_2SiO_5 + C + CH_4 + 5.95H_2 \quad (2)$$

Afterwards the formed carbon is consumed through reacting with water (Fig. 5(e) and (f)). Because CO_2 is the species with higher partial pressures than CO at temperatures below 900 °C (Fig. 2), the main carbon consuming reaction[37] should be:

$$C + H_2O = 1/2CO_2 + 1/2CH_4 \quad (3)$$

and

$$C + 2H_2O = CO_2 + 2H_2 \quad (4)$$

In addition, carbon also can be consumed by methane formation, but the reaction rate is extremely sluggish at low temperatures.[44]

As the equilibrium state is achieved, the dominating reaction between water and $Ti_3Si_{0.9}Al_{0.1}C_2$ is

$$Ti_3Si_{0.9}Al_{0.1}C_2 + 9.95H_2O = 3TiO_2 + 0.85SiO_2 + 0.05Al_2SiO_5 + CO_2 + CH_4 + 7.95H_2 \quad (5)$$

It should be noted that parts of the CO_2 are converted to CO with increasing water and temperature.

4.3. Effect of Al dopant

The effect of Al dopant includes: delaying the phase transformation from anatase to rutile, promoting the formation of carbon, the decomposition of $Ti_3Si_{0.9}Al_{0.1}C_2$ and the crystallization of silica.

Ding et al.[45] and Yang et al.[46] studied the effect of alumina dopant on the titania phase transformation. Both of them observed that the presence of a small amount of alumina in titania powder could effectively delay the phase transformation from anatase to rutile. Their results agree with our experiments.

As mentioned above, the production of carbon is attributed to the selective oxidative extraction of other elements, i.e. carbon comes from the decomposition of the substrate. Obviously, the easier the decomposition of $Ti_3Si_{0.9}Al_{0.1}C_2$, the easier the formation of carbon. The calculations indicate that the activity of Si and Al in the solid solution is higher than that of Si in Ti_3SiC_2,[41] which have been compellingly testified by the oxidation[18,19] and thermal stability experiments.[42,43] The formation of a continuous alumina layer on the surfaces of the $Ti_3Si_{0.9}Al_{0.1}C_2$ samples during oxidation confirms the high activity of Al,[18,19] especially considering the low content of Al in the substrate. In case of the thermal stability in nitrogen,[42,43] silicon and aluminum exhibited higher activity than that of titanium in $Ti_3Si_{0.9}Al_{0.1}C_2$ because they could combine with nitrogen to form Al(Si)N[42]; on the contrary, titanium displayed higher activity than that of silicon in Ti_3SiC_2 because TiN was formed as the final product.[43]

For layered ceramics Ti_3SiC_2, Ti_3AlC_2 and $Ti_3Si_{0.9}Al_{0.1}C_2$, the preferred decomposition mode is that Si/Al escapes from the substrate and leave TiC_x behind due to the high activity of Si and Al.[32,47–54] Since silicon and aluminum in the solid solution is more active, the decomposition process of $Ti_3Si_{0.9}Al_{0.1}C_2$ is certainly accelerated, which simultaneously promotes the formation of carbon. This result strongly indicates that bulk $Ti_3Si_{0.9}Al_{0.1}C_2$ may possess better hydrothermal oxidation resistance than that of Ti_3SiC_2. This prediction is testing now in our laboratory.

The reason for the promoting effect of alumina on the crystallization of silica is complicated and is not clear now, which is needed to be further investigated.

5. Conclusions

The hydrothermal oxidation of $Ti_3Si_{0.9}Al_{0.1}C_2$ displayed a two-step process involving at first the formation of carbon and oxides, such as TiO_2, SiO_2 and sillimanite/alumina, and then the consumption of the as-produced carbon to form carbon oxides and methane. The formation of carbon was due to the selectively oxidative extraction of titanium, silicon and aluminum from the substrate. Compared to Ti_3SiC_2, the hydrothermal oxidation behavior was obviously changed after adding aluminum dopant. The differences included: delaying the phase transformation from anatase to rutile, promoting the formation of carbon, the crystallization of silica and decomposition of $Ti_3Si_{0.9}Al_{0.1}C_2$. This behavior had a close relation with the weak interactions between Ti–Si and Ti–Al atomic layers and the layered structure of $Ti_3Si_{0.9}Al_{0.1}C_2$.

Acknowledgments

H.B. Zhang is grateful to the Alexander von Humboldt Foundation. We appreciate the experimental assistance of Mr. D. Russ of Tübingen University. This work was supported by DFG (Grants Ni 299/9 and Ni 299/13-1), the National Outstanding Young Scientist Foundation for Y.C. Zhou (Grant 59925208), Natural Science Foundation of China (Grants 50232040, 50302011, 50832008 and 90403027), '863' project and High-tech Bureau of the Chinese Academy of Sciences.

References

1. Nickel, K. G. and Seipel, B., Corrosion penetration monitoring of advanced ceramics in hot aqueous fluids. *Mater. Res.*, 2004, **7**, 1–9.
2. Gogotsi, Y. G., Nickel, K. G., Bahloul-Hourlier, D., Merle-Mejean, T., Khomenko, G. E. and Skjerlie, K. P., Structure of carbon produced by hydrothermal treatment of beta-SiC powder. *J. Mater. Chem.*, 1996, **6**, 595–604.
3. Jacobson, N. S., Gogotsi, Y. G. and Yoshimura, M., Thermodynamic and experimental study of carbon formation on carbides under hydrothermal conditions. *J. Mater. Chem.*, 1995, **5**, 595–601.
4. Gogotsi, Y. G., Kofstad, P., Yoshimura, M. and Nickel, K. G., Formation of sp3-bonded carbon upon hydrothermal treatment of SiC. *Diam. Relat. Mater.*, 1996, **5**, 151–162.
5. Kraft, T. and Nickel, K. G., Carbon formed by hydrothermal treatment of α-SiC crystals. *J. Mater. Chem.*, 2000, **10**, 671–680.
6. Kraft, T., Nickel, K. G. and Gogotsi, Y. G., Hydrothermal degradation of chemical vapour deposited SiC fibres. *J. Mater. Sci.*, 1998, **33**, 4357–4364.
7. Yoshimura, M., Kase, J. I. and Sōmiya, S., Oxidation of SiC powder by high-temperature, high-pressure H_2O. *J. Mater. Res.*, 1986, **1**, 100–103.
8. Kitaoka, S., Tsuji, T., Katoh, T., Yamaguchi, Y. and Sato, K., Tribological characteristics of Si_3N_4 ceramic in high-temperature and high-pressure water. *J. Am. Ceram. Soc.*, 1994, **77**, 580–588.
9. Oda, K., Yoshio, T., Miyamoto, Y. and Koizumi, M., Hydrothermal corrosion of pure, hot isostatically pressed silicon nitride. *J. Am. Ceram. Soc.*, 1993, **76**, 1365–1368.
10. Sudhir, B. and Raj, R., Effect of steam velocity on the hydrothermal oxidation/volatilization of silicon nitride. *J. Am. Ceram. Soc.*, 2006, **89**, 1380–1387.
11. Oda, K. and Yoshio, T., Hydrothermal corrosion of alumina ceramics. *J. Am. Ceram. Soc.*, 1997, **80**, 3233–3236.
12. Barsoum, M. W., The $M_{(N+1)}AX_{(N)}$ phases: a new class of solids; thermodynamically stable nanolaminates. *Prog. Solid. State Chem.*, 2000, **28**, 201–281.
13. Barsoum, M. W. and El-Raghy, T., Synthesis and characterization of a remarkable ceramic: Ti_3SiC_2. *J. Am. Ceram. Soc.*, 1996, **79**, 1953–1956.
14. Zhou, Y. C. and Sun, Z. M., Microstructure and mechanism of damage tolerance for Ti_3SiC_2 bulk ceramics. *Mater. Res. Innov.*, 1999, **2**, 360–363.
15. Low, I. M., Lee, S. K. and Lawn, B. R., Contact damage accumulation in Ti_3SiC_2. *J. Am. Ceram. Soc.*, 1998, **81**, 225–228.
16. Bao, Y. W., Zhou, Y. C. and Zhang, H. B., Investigation on reliability of nanolayer-grained Ti_3SiC_2 via Weibull statistics. *J. Mater. Sci.*, 2007, **42**, 4470–4475.
17. Zhang, H. B., Wang, X., Nickel, K. G. and Zhou, Y. C., Experimental and thermodynamic study of the hydrothermal oxidation behavior of Ti_3SiC_2 powders. *Scripta Mater.*, 2008, **56**, 746–749.
18. Zhou, Y. C., Zhang, H. B., Liu, M. Y., Wang, J. Y. and Bao, Y. W., Preparation of TiC free Ti_3SiC_2 with improved oxidation resistance by substitution of Si with Al. *Mater. Res. Innov.*, 2004, **8**, 97–102.
19. Zhang, H. B., Zhou, Y. C., Bao, Y. W. and Li, M. S., Improving the oxidation resistance of Ti_3SiC_2 by forming a $Ti_3Si_{0.9}Al_{0.1}C_2$ solid solution. *Acta Mater.*, 2004, **52**, 3631–3637.
20. Eriksson, G. and Hack, K., ChemSage—a computer program for the calculation of complex chemical equilibria. *Metall. Mater. Trans. B*, 1990, **21**, 1013–1023.
21. Zhou, Y. C., Sun, Z. M., Chen, S. Q. and Zhang, Y., In-situ hot pressing solid–liquid reaction synthesis of dense titanium silicon carbide bulk ceramics. *Mater. Res. Innov.*, 1998, **2**, 142–146.
22. Nakamizo, M., Kammereck, R. and Walker, P. L., Laser Raman studies on carbons. *Carbon*, 1974, **12**, 259–267.
23. Schwan, J., Ulrich, S., Batori, V., Ehrhardt, H. and Silva, S. R. P., Raman spectroscopy on amorphous carbon films. *J. Appl. Phys.*, 1996, **80**, 440–447.
24. Nikiel, L. and Jagodzinski, P. W., Raman spectroscopic characterization of graphites: a re-evaluation of spectra/structure correlation. *Carbon*, 1993, **31**, 1313–1317.
25. Lee, K. S. and Park, I. S., Anatase-phase titanium oxide by low temperature oxidation of metallic Ti thin film. *Scripta Mater.*, 2003, **48**, 659–663.
26. Ding, X. Z. and Liu, X. H., Correlation between anatase-to-rutile transformation and grain growth in nanocrystalline titania powders. *J. Mater. Res.*, 1998, **13**, 2556–2559.
27. Zhang, H. B., Zhou, Y. C., Bao, Y. W. and Wang, J. Y., Oxidation behavior of bulk Ti_3SiC_2 at intermediate temperatures in dry air. *J. Mater. Res.*, 2006, **21**, 402–408.
28. Grzmil, B., Kic, B. and Rabe, M., Inhibition of the anatase–rutile phase transformation with addition of K_2O, P_2O_5, and Li_2O. *Chem. Pap.*, 2004, **58**, 410–414.
29. Barsoum, M. W., El-Raghy, T. and Ogbuji, L. U. J. T., Oxidation of Ti_3SiC_2 in air. *J. Electrochem. Soc.*, 1997, **144**, 2508–2516.
30. Li, S. B., Cheng, L. F. and Zhang, L. T., Oxidation behavior of Ti_3SiC_2 at high temperature in air. *Mater. Sci. Eng. A*, 2003, **341**, 112–120.
31. Chen, T., Green, P. M., Jordan, J. L., Hampikian, J. M. and Thadhani, N. N., Oxidation of Ti_3SiC_2 composites in air. *Metall. Mater. Trans. A*, 2002, **33**, 1737–1742.
32. Racault, C., Langlais, F. and Naslain, R., Solid-state synthesis and characterization of the ternary phase Ti_3SiC_2. *J. Mater. Sci.*, 1994, **29**, 3384–3392.
33. Nguyena, T. D., Choia, J. H., Parkb, S. W. and Leea, D. B., Comments on the high temperature oxidation characteristics of Ti_3SiC_2 in air. *J. Ceram. Process. Res.*, 2007, **8**, 397–401.
34. Sun, Z. M., Zhou, Y. C. and Li, M. S., Oxidation behaviour of Ti_3SiC_2-based ceramic at 900–1300 °C in air. *Corros. Sci.*, 2001, **43**, 1095–1109.
35. Gao, N. F., Miyamoto, Y. and Zhang, D., On physical and thermochemical properties of high-purity Ti_3SiC_2. *Mater. Lett.*, 2002, **55**, 61–66.
36. Yang, S. L., Sun, Z. M., Hashimoto, H., Park, Y. H. and Abe, T., Oxidation of Ti_3SiC_2 at 1000 °C in air. *Oxid. Met.*, 2003, **59**, 155–165.
37. Zhang, H, B., Effect of Al on synthesis and high-temperature properties of ternary ceramic Ti_3SiC_2. *PhD Thesis*, Institute of Metal Research, Chinese Academy of Sciences, Shenyang, China, 2006.
38. Shimada, S., Interfacial reaction on oxidation of carbides with formation of carbon. *Solid State Ionics*, 2001, **141**, 99–104.
39. Shimada, S., Oxidation and mechanism of single crystal carbides with formation of carbon. *J. Ceram. Soc. Jpn.*, 2001, **109**, S33–S42.

40. Wu, E. D., Wang, J. Y., Zhang, H. B., Zhou, Y. C., Sun, K. and Xue, Y. J., Neutron diffraction studies of $Ti_3Si_{0.9}Al_{0.1}C_2$ compound. *Mater. Lett.*, 2005, **59**, 2715–2719.
41. Wang, J. Y. and Zhou, Y. C., First-principles study of equilibrium properties and electronic structure of $Ti_3Si_{0.75}Al_{0.25}C_2$ solid solution. *J. Phys.: Condens. Matter*, 2003, **15**, 5959–5968.
42. Zhang, H. B., Zhang, J., Zhou, Y. C., Bao, Y. W. and Li, M. S., Synthesis of AlN nanowires by nitridation of $Ti_3Si_{0.9}Al_{0.1}C_2$ solid solution. *J. Mater. Res.*, 2007, **22**, 561–564.
43. Zhang, H. B., Zhou, Y. C., Bao, Y. W. and Li, M. S., Titanium silicon carbide pest induced by nitridation. *J. Am. Ceram. Soc.*, 2008, **91**, 494–499.
44. Schröder, F., Gmelins Handbuch der Anorganischen Chemie, Kohlenstoff Teil B Lieferung 3, 1968.
45. Ding, X. Z., Liu, L., Ma, X. M., Qi, Z. Z. and He, Y. Z., The influence of alumina dopant on the structural transformation of gel-derived nanometer titania powders. *J. Mater. Sci. Lett.*, 1994, **13**, 462–464.
46. Yang, J., Huang, Y. X. and Ferreira, J. M. F., Inhibitory effect of alumina additive on the titania phase transformation of a sol–gel-derived powder. *J. Mater. Sci. Lett.*, 1997, **16**, 1933–1935.
47. Low, I. M., Manurung, P., Smith, R. I. and Lawrence, D., A novel processing method for the microstructural design of functionally-graded ceramic composites. *Key Eng. Mater.*, 2002, **224–226**, 465–470.
48. Low, I. M., Depth profiling of phase composition in a novel Ti_3SiC_2–TiC system with graded interfaces. *Mater. Lett.*, 2004, **58**, 927–932.
49. Barsoum, M. W., El-Raghy, T., Farber, L., Amer, M., Christini, R. and Adams, A., The topotactic transformation of Ti_3SiC_2 into a partially ordered cubic $Ti(C_{0.67}Si_{0.06})$ phase by the diffusion of Si into molten cryolite. *J. Electrochem. Soc.*, 1999, **146**, 3919–3923.
50. El-Raghy, T., Barsoum, M. W. and Sika, M., Reaction of Al with Ti_3SiC_2 in the 800–1000 °C temperature range. *Mater. Sci. Eng. A*, 2001, **298**, 174–178.
51. El-Raghy, T. and Barsoum, M. W., Diffusion kinetics of the carburization and silicidation of Ti_3SiC_2. *J. Appl. Phys.*, 1998, **83**, 112–119.
52. Emmerlich, J., Music, D., Eklund, P., Wilhelmsson, O., Jansson, U., Schneider, J. M. *et al.*, Thermal stability of Ti_3SiC_2 thin films. *Acta Mater.*, 2007, **55**, 1479–1488.
53. Wang, X. H. and Zhou, Y. C., Stability and selective oxidation of aluminum in nano-laminate Ti_3AlC_2 upon heating in argon. *Chem. Mater.*, 2003, **15**, 3716–3720.
54. Chen, J. X., Zhou, Y. C., Zhang, H. B., Wan, D. T. and Liu, M. Y., Thermal stability of Ti_3AlC_2/Al_2O_3 composites in high vacuum. *Mater. Chem. Phys.*, 2007, **104**, 109–112.